Discovery of novel, potent, selective and cellular active ADC type PTP1B inhibitors via fragment-docking-oriented de novel design

Yongli Du [a,*,†], Hao Ling [a,†], Meng zhang [c], Jingkang Shen [b], Qunyi Li [d,*]

[a] School of Chemistry and Pharmaceutical Engineering, Qilu University of Technology, 3501 Daxue Road, Jinan 250353, China
[b] State Key Laboratory of Drug Research, Shanghai Institute of Materia Medica, Chinese Academy of Sciences, 555 Zu Chong Zhi Road, Shanghai 201203, China
[c] Brunswick Laboratories (China), 5 Xing Han Road, Suzhou 215021, China
[d] Clinical Pharmacy Laboratory, Huashan Hospital, Fudan University, 12 Wu Lu Mu Qi M Road, Shanghai 200040, China

ARTICLE INFO

ABSTRACT

Fragment-docking-oriented de novel design for both the catalytic site and the C phosphotyrosine binding site led to the discovery of novel scaffold and chemical easy N-(2,5-diethoxy-phenyl)-methanesulfon-amide based phosphotyrosine mimetics that when incorporated into ureas are high potent and selective inhibitors of protein tyrosine phosphatase 1B. Among them, compound **15** was shown to be the most potent PTP1B inhibitor with great selectivity over the highly homologous T-cell protein tyrosine phosphatase.

© 2015 Published by Elsevier Ltd.

1. Introduction

Protein tyrosine phosphatase 1B (PTP1B) is a negative regulator of the insulin and leptin receptor pathways.[1–3] PTP1B deficient mice were viable, healthy, and lean and they displayed enhanced insulin sensitivity and resistance to diet-induced obesity.[4,5] This provides important evidence that PTP1B inhibition would be an effective diabetes therapy. It has been extensively studied within academia and the pharmaceutical industry and is regarded by many as one of the best validated drug targets for intervention in type 2 diabetes and obesity.

However, there is no drug approved as PTP1B inhibitor until now, and only two small molecule PTP1B inhibitors entered clinical trials. Nearly all medicinal chemistry efforts have been severely hindered because the potent phosphotyrosine (pTyr) mimetics, such as bioisosteric nonhydrolyzable DFMP pTyr mimetics,[7,8] carboxylic or dicarboxylic acid pTyr mimetics,[10–13] heterocyclic TDZ and IZD pTyr mimetics,[6,14,15] are negatively charged with poor membrane permeability and low selectivity.[4,9]

The crystal structure of PTP1B in complex with the IR kinase activation segment revealed that the large, negatively charged substrate interacts with multiple positively charged sites in the protein (A, B, C, D and E).[16] The A site is the catalytic pocket of the enzyme where phosphotyrosine (Tyr) residues of the IR kinase activation peptide are dephosphorylated. The A site is 9-Å deep (from Cys215 to Phe182) and 10-Å wide (from Tyr46 to Gln262). Its lower half contains the polar phosphate binding loop (Cys215–Arg221) and the catalytic Cys215. Its upper half contains hydrophobic residues (Y46, V49, F182, A217, I219, and Q262) that interact with the aryl ring of pTyr. The D site is a small narrow pocket, partially shielded from solvent and lined with polar and charged residues (Tyr46, Glu115, Lys120, Asp181, and Ser216). The most desirable aspect of building into this site is the possibility of increasing potency. The C site is highly solvent exposed and completely flat except for Lys41 and Arg47, and it shares Tyr46 and Asp48 with the A site.[17]

In our pursuit to discover novel potent and selective PTP1B inhibitors, N-(2,5-diethoxy-phenyl)-methanesulfonamide based pTyr mimetics were identified through fragment-docking-oriented de novel design. Here we report the discovery of the design, synthesis and bioactivity of the novel, potent, selective and cellular active PTP1B inhibitors which interact with the A, D and C site, namely ADC type PTP1B inhibitors.

* Corresponding authors. Tel.: +86 531 89631208; fax: +86 0531 89631207 (Y.D.); tel.: +86 21 52889303; fax: +86 21 52889307 (Q.L.).

E-mail addresses: ylduyjs@163.com (Y. Du), qyli1234@163.com (Q. Li).

† These two authors contributed equally to this work.

2. Inhibitor design

Our efforts toward the design of PTP1B inhibitors started with the analysis of the interactions between PTP1B and its ligand compound **1** (K_i = 1.7 nM, Fig. 1) in the X-ray crystal (PDB code 2CNE). The DFMP moiety of compound **1** (gray capped sticks, Fig. 2) binds at the center of the phosphate binding loop (ball and stick) through multiple hydrogen-bonding interactions with the catalytic residue in the A site, the C-terminal amide and adjacent amide NHs hydrogen bond (yellow dashed lines) to the carboxylate of Asp48 at the A–C border, the distal amide CO hydrogen bonds to the backbone NH of Arg47 and the distal DFMP interacts with Lys41 and Arg47 in the C site.[18]

We envisioned that suitable hydrogen bond acceptors instead of negatively charged phosphoric acid groups in pTyr mimetics for hydrogen binding to the catalytic residues in A site, maybe demonstrate potent affinity and good membrane permeability. Closer inspection and chemical intuition suggested that neutral methyl sulfonyl fragment **3** (Fig. 3), probably forming multiple hydrogen-bonding interactions with the catalytic residues in the deep A site, maybe effectively mimic the interactions of DFMP **2** (Figs. 2 and 3) containing ligands. Docking simulations of the proposed compound **3** within the ADC site of PTP1B (PDB entry 2CNE) have been performed using Surflex docking program (Sybyl X 1.0) with the default setting. Molecular docking result showed that the two sulfonyloxygens in compound **3** hydrogen bond to Ser216, Arg221 and Ile219, similar to the phosphate group, in addition to Gly220 (Fig. 4).

Interacting with Asp48 on the outer edge of the pocket A has been shown to increase selectivity.[18] So the urea group having 1,3-double-NHs was introduced to methyl sulfonyl containing fragment **3** for interacting with the carboxylate of Asp48. The docking structure of methyl sulfonyl fragment **3** and DFMP containing ligand **1** suggested that a one-atom linker off the para position of the phenyl ring in fragment **3** should be optimal for linking with the urea group, thus fragment **4** (Fig. 2) was designed. Docking studies showed that fragment **4** formed a network of H-bonds with Arg221, Gy220 and Ile219, little different from fragment **3**, and hydrogen-bonding interactions of –NH present at urea group have also been observed with carboxylate of Asp48 (Fig. 5).

The most desirable aspect of building into D site is the possibility of increasing potency. The advantage of interacting with hydrophobic residues (Val49, Phe52, Ile219, and Met258) proximal to the A site is the possibility of simultaneously increasing affinity and specificity.[17] Docking results suggested that a three-atom group at 2 and 5 position of the phenyl ring in fragment **4** should be optimal for interact with the D site and the hydrophobic residues (Val49, Phe52, Ile219, and Met258). Guided by docking results, compound **12** (Fig. 2) was designed. Molecular docking simulation studies of compound **12** displayed the same binding mode to compound **4** (Fig. 5). As expected, the 2-ethoxy group pointed to the D site and the 5-ethoxy group pointed to the hydrophobic residues (Val49, Phe52, Ile219, and Met258). The scoring results suggested compound **12** was favorable than fragments **3** and **4** in binding energy. We postulated that the neutral *N*-(2,5-diethoxy-phenyl)-methanesulfonamide containing compound **12** may provide improved membrane permeability compared to the hard charged phosphonates containing inhibitors. Thus compound **12** and its analogs were chosen as our initial synthetic targets.

3. Chemistry

The syntheses of aromatic β-amino-ketone analogs **12**–**18** were accomplished as depicted in Scheme 1. Starting from material **5**,
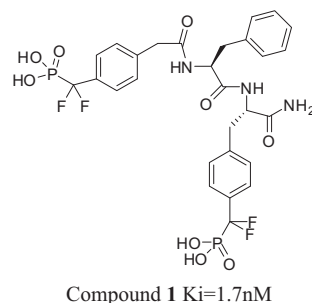

Compound 1 Ki=1.7nM

Figure 1. Previously reported difluoromethylphosphonic acid (**DFMP**) derivative.
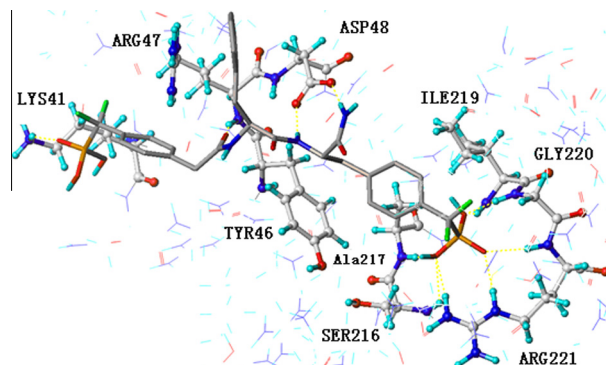

Figure 2. Compound **1** (Gray) was docked into PTP1B crystal structure (2CNE). Hydrogen bonding interactions are shown with dotted yellow lines. These images were generated using the Sybyl-x program.

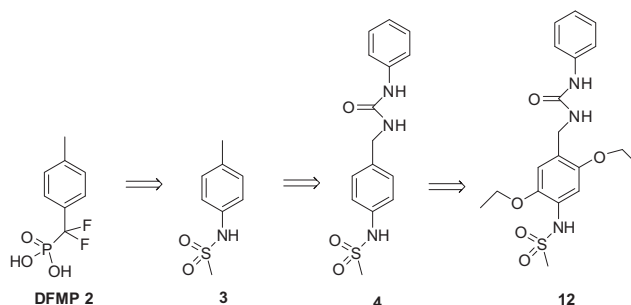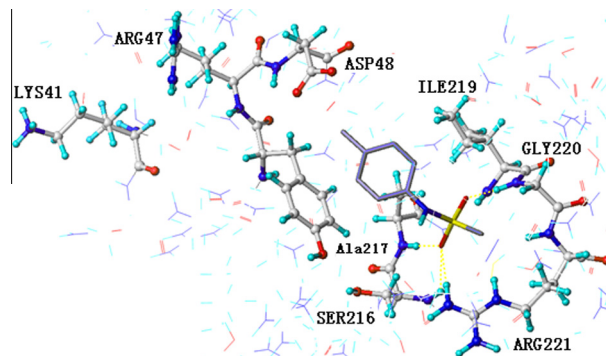**Figure 3.** Fragments design and growth of PTP1B inhibitor.

Figure 4. Docking model of fragment **3** (blue) on the A site of PTP1B (PDB code 2CNE). Hydrogen bonding interactions are shown with dotted yellow lines. These images were generated using the Sybylx program.

intermediate **6** was synthesized through alkylation with bromoethane.[19] Then intermediate **7** was produced through nitration

ARTICLE IN PRESS

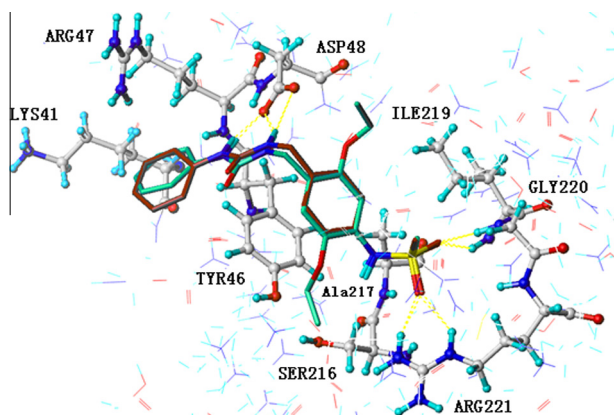*Y. Du et al./Bioorg. Med. Chem. xxx (2015) xxx–xxx*

3

Figure 5. Superimposition of docking model of fragment **4** (red) and compound **12** (green) on the ADC site of PTP1B (PDB code 2CNE). Hydrogen bonding interactions are shown with dotted yellow lines. These images were generated using the Sybyl-x program.

reaction with HNO_3 and acetic acid in good yield.[20] After bromination and amination, intermediate **7** was converted to intermediate **10**.[21,22] Intermediate **11** was obtained in high yield by condensing benzylamine intermediate **10** with phenyl chloroformate.[23,24] The intermediate **11** effectively reacts with various amines to give the corresponding N-benzyl urea intermediates **12H–18H** in excellent yields.[23,24] Intermediates **13I–18I** were prepared through the reduction of nitro intermediates.[25] Methanesulfonyl chloride was condensed with Intermediates **13I–18I** separately to give compound **12–18**.

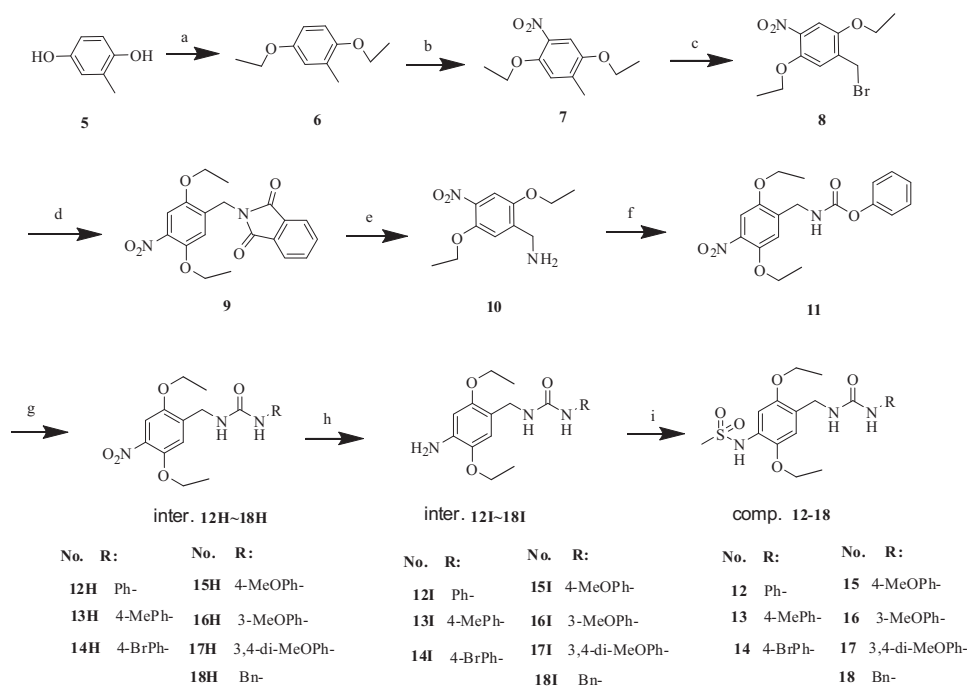## 4. Results and discussion

This is the first attempt to develop neutral N-(2,5-diethoxyphenyl)-methanesulfonamide containing compounds as potential pTyr mimetics to improve PTP1B inhibition, selectivity. Initially,
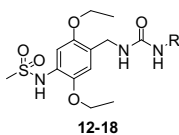
compound **12** was synthesized and identified to posses potent inhibition activity ($IC_{50} = 537$ nM, Table 1) against the PTP1B enzyme. The potent activity of compound **12** proved the rationality of our design strategy above. Replacement of the 3-phenyl group on ureido (**12**) with a benzyl group in **18** ($IC_{50} = 756$ nM, Table 1) resulted in a dramatic decrease in inhibition activity against the PTP1B enzyme. The docking structure of PTP1B/**18** (Fig. 6) reveals that the aryl ring of 3-benzyl group on urea does not interact significantly with the protein but instead pointing out of the pocket.

Next, N-{2,5-diethoxy-4-[(3-phenyl-ureido)-methyl]-phenyl}-methanesulfonamide was chosen as general structure and a number of substituted phenyl-ureido analogs (e.g., **13–17**, Table 1) were synthesized to study the preliminary structure–activity relationships. 4-methoxy analog (**15**, $IC_{50} = 203$ nM), 4-methyl analog (**13**, $IC_{50} = 309$ nM) and 4-bromoanalog (**14**, $IC_{50} = 212$ nM) all displayed improved PTP1B inhibition activity than compound **12**. This probably because the introduction of hydrophobic group on 4 position of phenyl enhanced the hydrophobic interactions between compounds **13–15** and the residues in C site of PTP1B. However, replacement of the 4-methoxy group (**15**) with a 3-methoxy group in **16** ($IC_{50} = 2733$ nM) resulted in a dramatic decrease (10-fold) in PTP1B inhibition activity. Interestingly, when introducing methoxy group on both 3 and 4 position of phenyl group (**17**, $IC_{50} = 204$ nM) still displayed potent inhibition activity, similar to analog **15**, against the PTP1B enzyme.

Potent active compounds (**13**, **14**, **15**) were selected to test against a panel of PTPs including homologous T-cell protein tyrosine phosphatase (TCPTP), SHP1, SHP2 and the receptor-like PTPs, LAR. As shown in Table 2, all these inhibitors demonstrated excellent PTP1B selectivity over other PTPs. No inhibition of SHP2 and LAR was observed at 25 μM in the three tested compounds. No inhibition of SHP1 was observed in compound **13**. 10-fold and 40-fold selectivity for PTP1B over SHP1 was observed separately in compound **14** and **15**. Excitingly, compounds **13** (16-fold) and **14** (6-fold) displayed good PTP1B selectivity over TCPTP, and the most potent compound **15** demonstrated more than 120 times selectivity for PTP1B over the highly homologous TCPTP.

No.	R:	No.	R:	No.	R:	No.	R:	No.	R:	No.	R:
12H	Ph-	15H	4-MeOPh-	12I	Ph-	15I	4-MeOPh-	12	Ph-	15	4-MeOPh-
13H	4-MePh-	16H	3-MeOPh-	13I	4-MePh-	16I	3-MeOPh-	13	4-MePh-	16	3-MeOPh-
14H	4-BrPh-	17H	3,4-di-MeOPh-	14I	4-BrPh-	17I	3,4-di-MeOPh-	14	4-BrPh-	17	3,4-di-MeOPh-
		18H	Bn-			18I	Bn-			18	Bn-

Scheme 1. Reagents and conditions for the synthesis of compounds **12–18**: (a) EtBr, K_2CO_3, DMF, 80 °C, 12 h; (b) HNO_3, AcOH, rt, 3 h; (c) NBS, BPO, CCl_4, 80 °C, 10 h; (d) phthalimidepotassium, TBAB, MeOH, 80 °C, 0.5 h; (e) $N_2H_4 \cdot H_2O$, MeOH, reflux, 4 h; (f) Carbonochloridic acid, phenyl ester, Et_3N, DCM; (g) Et_3N, dioxane, 80 °C, 8 h; (h) $NiCl_2 \cdot 6H_2O$, $NaBH_4$, MeOH, rt, 0.5 h; (i) methanesulfonyl chloride, DCM, N_2, pyridine, rt, 8 h.

ARTICLE IN PRESS

4   Y. Du et al./Bioorg. Med. Chem. xxx (2015) xxx–xxx

Table 1
Inhibitory activity of compounds **12–18** against PTP1B[a]

12-18

| Compound	R	IC$_{50}$(nM) mean ± SEM
Control	Oleanolic acid	2058 ± 202
12	Ph-	537 ± 42
13	4-MePh-	309 ± 99
14	4-BrPh-	212 ± 57
15	4-MeOPh-	203 ± 79
16	3-MeOPh-	2733 ± 23
17	3,4-di-MeO-Ph-	204 ± 19
18	Bn-	756 ± 115

[a] Values represent triplicate determinations.
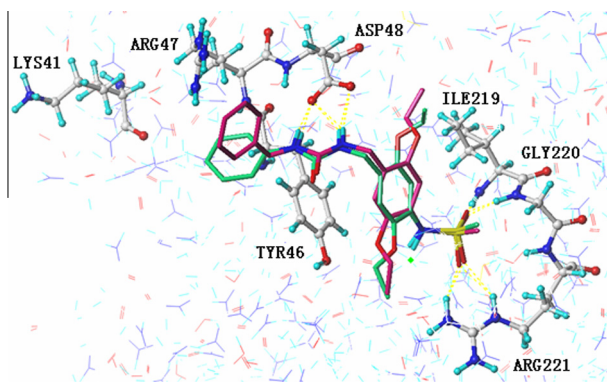
Figure 6. Superimposition of docking model of compounds **12** (green) and **18** (pink) on the A, D and C sites of PTP1B (PDB code 2CNE). Hydrogen bonding interactions are shown with dotted yellow lines. These images were generated using the Sybyl-x program.

The effect of compound **15** on the kinetic profile of PTP1B-catalyzed pNPP hydrolysis was investigated as described in methods. As shown in Table 3, with the increasing concentrations of compound **15**, the K_m value of PTP1B increased accordingly. However, the V_{max} value of PTP1B remained almost constant. The kinetic parameters presented in Table 3 suggested that compound **15** acted as a competitive PTP1B inhibitor. Further analysis by Lineweaver-Burk plot also demonstrated the competitive inhibitory mechanism of **15** on PTP1B (Fig. 7). Kinetic analysis of enzymatic reaction suggested **15** was a competitive PTP1B inhibitor.

It has been suggested that the intrinsic tyrosine kinase activity of the IRβ plays a pivotal role in insulin-mediated signaling cascades.[26] PTP1B participates in the dephosphorylation and inactivation of IR, thus attenuating insulin signaling.[26] Several studies indicates that inhibition of PTP1B by specific antisense oligonucleotide[27] or inhibitors[28,29] results in improvement of

Table 3
The kinetic parameters of PTP1B enzyme in the pNPP hydrolysis in the presence of different concentrations of the inhibitor **15** LingH5[a]

Inhibitor (μM)	K_m (mM)	V_{max} (mOD/min)
0	1.81	57.97
0.1	2.96	58.34
0.2	3.89	54.79
0.4	4.52	48.92
0.8	7.32	52.49

[a] K_m is the Michaelis constant, V_{max} is the maximum rate and were calculated from the Michaelis–Menten equation.
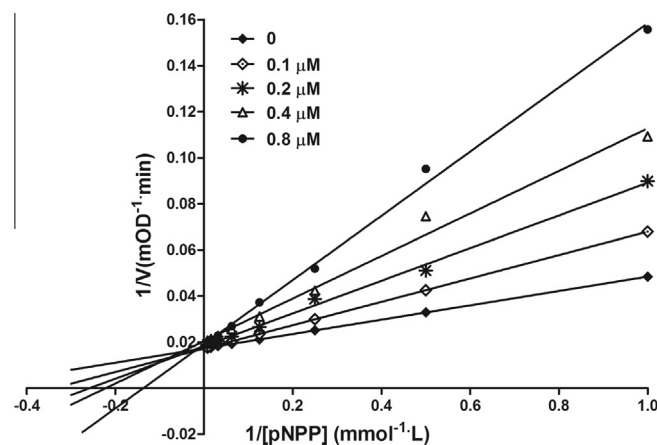
Figure 7. Representative competitive inhibitory effect of compound **15** on PTP1B-catalyzed pNPP hydrolysis. Data were shown by Lineweaver–Burk plot.
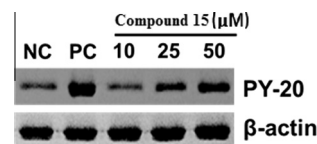
Figure 8. Effect of compound **15** on tyrosine phosphorylation of insulin receptor β (IRβ) in CHO cells transfected with hIRβ-expressing plasmid. NC, negative control; PC, positive control.

hyperglycaemia and insulin sensitivity in diabetic animal models. Thus, we evaluated the effects of compound **15** on phosphorylation level of IRβ in CHO cells transfected with hIRβg plasmid. As shown in Figure 8, compound **15** greatly enhanced insulin-mediated IRβ phosphorylation at concentrations of 25 μM and 50 μM.

5. Conclusion

The novel potent and selective PTP1B inhibitors, N-(2,5-diethoxy-phenyl)-methanesulfonamide based phosphotyrosine mimetics, were discovered through fragment-docking-oriented de novo design for the A, D and C site of PTP1B. Efficient syntheses

Table 2
The inhibitory activity of select compounds **13**, **14**, **15** as PTP1B inhibitors against a panel of PTPs, IC$_{50}$[a]

Compd	PTP1B (nM)	TCPTP (μM)	SHP1 (μM)	SHP2 (μM)	LAR (μM)
Oleanolic acid	1536 ± 267	5.46 ± 0.74			
Na$_3$VO$_4$			14.19 ± 2.63	11.62 ± 2.84	22.31 ± 4.67
13	309 ± 99	5.19 ± 0.64	NA[b]	NA	NA
14	212 ± 57	1.36 ± 0.27	2.31 ± 0.44	NA	NA
15	203 ± 79	NA	9.08 ± 1.26	NA	NA

[a] The pNPP assay. IC$_{50}$ values were determined by regression analysis and expressed as means ± SD of three replications.
[b] NA: Inhibition rate <50% at 25 μM concentration.

ARTICLE IN PRESS

Y. Du et al. / Bioorg. Med. Chem. xxx (2015) xxx–xxx

5

were established to provide *N*-(2,5-diethoxy-phenyl)-methanesulfonamide derivatives. The SAR study revealed that compound **15**, acting as a competitive inhibitor, was the most potent (IC_{50} = 203 nM) PTP1B inhibitor with great selectivity (more than 120-fold) over the highly homologous TCPTP. Interestingly, compound **15** displayed distinct cellular activity in enhancing insulin-mediated IRβ phosphorylation.

These *N*-(2,5-diethoxy-phenyl)-methanesulfonamide based ADC type phosphotyrosine mimetics provide novel scaffold and opportunities for the discovery of such PTP1B inhibitors in the future. Further optimization of these novel scaffold PTP1B inhibitors will be described in our next reports.

6. Experimental section

6.1. Chemistry

General synthetic methods: Unless otherwise noted, all materials were obtained from commercial suppliers and used without further purification. All reactions were monitored using thin-layer chromatography (TLC) on silica gel plates. NMR spectra were determined using a Bruker AVANCE II 400 spectrometers in $CDCl_3$ or DMSO solution. Elemental analyses were performed on a Der CHNOS Elementar Analysen-systemeVario EL III.

6.1.1. 1,4-Diethoxy-2-methyl-benzene (6) and 1,4-diethoxy-2-methyl-5-nitro-benzene (7)

2-Methyl-benzene-1,4-diol (**5**, 10.0 g, 80.55 mmol) was dissolved in dry *N,N*-dimethyl formamide. After addition of K_2CO_3 (33.5 g, 242.8 mmol), the solution was heated under nitrogen at 80 °C for 10 min, bromoethane (26.3 g, 241.7 mmol) was added dropwise to the solution over 30 min, followed by stirring at 80 °C for 12 h. Then the mixture was cooled to room temperature and *N,N*-dimethylformamide was removed by distillation. The residue was dissolved in dichloromethane and extracted with water (3 × 200 mL). The combined organic phases were dried with Na_2SO_4, and concentrated under reduced pressure to give the crude product **6** 8.8 g (yield 60.7%) without further purification.

1,4-Diethoxy-2-methyl-benzene (**6**, 8.0 g, 44.4 mmol), was dissolved in acetic acid (100 mL), and then the HNO_3 (11.3 mL, 178.0 mmol), was added to the solution and the mixture was stirred at room temperature for 3 h. Acetic acid was then removed by distillation. The residue was dissolved in dichloromethane and extracted with water (3 × 200 mL). The combined organic phases were dried with Na_2SO_4 and concentrated under reduced pressure. The remaining solid was recrystallized from methanol to give pure product **7** 8.2 g (yield 82%) of yellow solid. ^1H NMR (400 MHz, $CDCl_3$) δ 7.35 (s, 1H), 6.89 (s, 1H), 4.14 (q, *J* = 7.0 Hz, 2H), 4.03 (q, *J* = 6.9 Hz, 2H), 2.28 (s, 3H), 1.45 (dd, *J* = 12.9, 6.8 Hz, 6H).

6.1.2. Bromomethyl-2,5-diethoxy-4-nitro-benzene (8)

1,4-Diethoxy-2-methyl-5-nitro-benzene (**7**, 7.0 g, 31.1 mmol) was dissolved in carbon tetrachloride (150 mL). After addition of benzoyl peroxide (75 mg, 0.3 mmol), the mixture was heated at 80 °C for 10 min, *N*-bromosuccinimide (5.54 g, 31.1 mmol) was added to the solution, followed by stirring at 80 °C for 10 h. Then the mixture was cooled to room temperature and carbon tetrachloride was removed by distillation. The residue was dissolved in dichloromethane and extracted with water (3 × 200 mL). The combined organic phases were dried with Na_2SO_4, and concentrated under reduced pressure. The crude product was purified by flash column chromatography to give pure product **8** 8.5 g (yield 89.9%) of yellow solid. ^1H NMR (400 MHz, $CDCl_3$) δ 7.38 (s, 1H), 7.11 (s, 1H), 4.52 (s, 2H), 4.20–4.09 (m, 4H), 1.48 (dd, *J* = 13.0, 6.9 Hz, 6H).

6.1.3. 2-(2,5-Diethoxy-4-nitro-benzyl)-isoindole-1,3-dione (9)

Bromomethyl-2,5-diethoxy-4-nitro-benzene (**8**, 8.0 g, 26.3 mmol), potassium phthalimide (4.87 g, 26.3 mmol) and tetrabutylammonium bromide (84.7 mg, 0.026 mmol) were mixed in methanol and heated to 80 °C for 0.5 h. Then the mixture was cooled to room temperature and the precipitate were collected by filtration and dried to give the pure product **9** 8.5 g (yield 87.4%) of white solid. ^1H NMR (400 MHz, $CDCl_3$) δ 7.89 (dt, *J* = 6.9, 3.5 Hz, 2H), 7.80–7.75 (m, 2H), 7.36 (s, 1H), 7.04 (s, 1H), 4.93 (s, 2H), 4.08 (dq, *J* = 20.6, 7.0 Hz, 4H), 1.42 (td, *J* = 7.0, 2.9 Hz, 6H).

6.1.4. N-{4-[3-(4-Bromo-phenyl)-ureidomethyl]-2,5-diethoxy-phenyl}-methanesulfonamide (14)

2-(2,5-Diethoxy-4-nitro-benzyl)-isoindole-1,3-dione (**9**, 8.0 g, 21.6 mmol) was dissolved in methanol (120 mL) and the mixture was heated at 80 °C for 10 min. Then hydrazine hydrate (1.93 g, 30.9 mmol) was added to the solution followed by stirring at 80 °C for 4 h. Then the mixture was cooled to room temperature and methanol was removed by distillation. The solid residue was dissolved in dichloromethane (200 mL) and treated with aqueous 20% NaOH (200 mL). The aqueous phase was separated, extracted with dichloromethane (3 × 200 mL). The combined organic phases were dried with Na_2SO_4, and concentrated under reduced pressure. The crude was purified by flash column chromatography to give pure product **10** 4.7 g (yield 92.5%) of yellow solid.

2,5-Diethoxy-4-nitro-benzylamine (**10**, 0.40 g, 1.67 mmol) was dissolved in dichloromethane. after addition of carbonochloridic acid phenyl ester (0.287 g, 1.84 mmol) and triethylamine (0.186 g, 1.84 mmol), the mixture stirring at room temperature for 0.5 h. Dichloromethane was then removed by distillation. The residue was dissolved in dichloromethane and extracted with water (3 × 100 mL). The combined organic phases were dried with Na_2SO_4, and concentrated under reduced pressure. The crude was purified by flash column chromatography to give pure product **11** 0.518 g (yield 86.3%) of yellow solid.

(2,5-Diethoxy-4-nitro-benzyl)-carbamic acid phenyl ester (**11**, 0.4 g, 1.11 mmol) was dissolved in dioxane after addition of 1-amino-4-bromobenzene (0.191 g, 1.1 mmol) and triethylamine (1.12 g, 11.1 mmol). The mixture was heated at 80 °C for 8 h. Then the mixture was cooled to room temperature and dioxane was removed by distillation. The residue was dissolved in dichloromethane and extracted with water (3 × 100 mL). The combined organic phases were dried with Na_2SO_4, and concentrated under reduced pressure. The remaining solid was recrystallized from methanol to give pure product 1-(4-bromo-phenyl)-3-(2,5-diethoxy-4-nitro-benzyl)-urea (**14H**) 0.44 g (yield 90.5%), pale yellow solid. A mixture of 1-(4-bromo-phenyl)-3-(2,5-diethoxy-4-nitro-benzyl)-urea (**14H**, 400 mg, 0.91 mmol), $NiCl_2 \cdot 6H_2O$ (371 mg, 1.56 mmol), $NaBH_4$ (119 mg, 3.12 mmol), and MeOH was stirring at room temperature for 0.5 h. The mixture was made acidic with a 10% HCl solution and extracted with Ethyl acetate, the organic layer was washed with a saturated NaCl solution (3 × 100 mL), the combined organic phases were dried with Na_2SO_4, and concentrated under reduced pressure. The product was purified by flash column chromatography to give pure product 1-(4-amino-2,5-diethoxy-benzyl)-3-(4-bromo-phenyl)-urea (**14I**) 0.3 g (yield 80.5%), white solid. 1-(4-amino-2,5-diethoxy-benzyl)-3-(4-bromo-phenyl)-urea (**14I**, 260 mg, 0.64 mmol) was dissolved in dichloromethane after addition of pyridine (56 mg, 0.70 mmol). The solution was stirring at room temperature for 10 min and methanesulfonyl chloride (73 mg, 0.64 mmol) was added dropwise to the solution, followed by stirring at room temperature for 8 h. Dichloromethane was then removed by distillation. The solid residue was dissolved in dichloromethane (50 mL) and washed with a saturated NaCl solution (3 × 100 mL). The combined organic

ARTICLE IN PRESS

6
Y. Du et al./Bioorg. Med. Chem. xxx (2015) xxx–xxx

phases were dried with Na_2SO_4 and concentrated under reduced pressure. The crude product was purified by flash column chromatography to give pure product (**14**) 0.17 g (yield 54.8%) of white solid. ^{1}H NMR (400 MHz, DMSO) δ 8.85 (s, 1H), 8.73 (s, 1H), 7.44–7.27 (m, 4H), 6.94 (s, 1H), 6.87 (s, 1H), 6.42 (t, $J = 6.0$ Hz, 1H), 4.21 (d, $J = 5.6$ Hz, 2H), 3.98 (q, $J = 6.8$ Hz, 4H), 2.92 (s, 3H), 1.32 (dd, $J = 12.0, 6.4$ Hz, 6H). ^{13}C NMR (101 MHz, DMSO) δ 154.90, 149.65, 145.37, 139.86, 131.30(2C), 125.97, 125.23, 119.55(2C), 113.72, 112.30, 110.55, 64.61, 64.12, 40.20, 38.12, 14.67, 14.61. Anal. ($C_{19}H_{24}N_3O_5SBr$): Anal. Calcd for C, 46.92; H, 4.97; N, 8.64; S, 6.59. Found: C, 47.41; H, 4.95; N, 8.74; S, 6.49.

6.1.5. N-{2,5-Diethoxy-4-[(3-phenyl-ureido)-methyl]-phenyl}-methanesulfonamide (12)

According to the same procedure described for **14H**, **11** (500 mg, 1.39 mmol) was treated with aniline (129 mg, 1.39 mmol) and triethylamine (1.40 g, 13.9 mmol) to afford 400 mg (yield 80.0%) of 1-(2,5-diethoxy-4-nitro-benzyl)-3-phenyl-urea (**12H**) as a white solid. According to the same procedure described for **14I**, **12H** (360 mg, 1.0 mmol) was treated with $NiCl_2 \cdot 6H_2O$ (408 mg, 1.7 mmol) and $NaBH_4$ (129 mg, 3.4 mmol) to afford 285 mg (86.4%) of 1-(4-amino-2,5-diethoxy-benzyl)-3-phenyl-urea (**12I**) as a white solid. According to the same procedure described for **14**, **12I** (260 mg,0.72 mmol) was treated with pyridine (62.9 mg, 0.80 mmol) and methanesulfonyl chloride (82.4 mg, 0.72 mmol) to afford 180 mg (yield 60.0%) of N-{2,5-diethoxy-4-[(3-phenyl-ureido)-methyl]-phenyl}-methanesulfonamide (**12**) as a white solid. ^{1}H NMR (400 MHz, CDCl$_3$) δ 7.26 (s, 3H), 7.06 (d, $J = 9.1$ Hz, 2H), 6.88 (s, 1H), 6.76 (s, 1H), 4.36 (s, 2H), 4.02–3.92 (m, 4H), 2.91 (s, 3H), 1.32 (m, 6H). ^{13}C NMR (101 MHz, DMSO) δ 155.11, 149.66, 145.38, 140.43, 128.57 (2C), 126.16, 125.19, 121.02, 117.70(2C), 113.72, 110.56, 64.62, 64.13, 40.21, 38.08, 14.67, 14.61; Anal. ($C_{19}H_{25}N_3O_5S$): Anal. Calcd for C, 56.00; H, 6.18; N, 10.31; S, 7.87. Found: C, 56.11; H, 6.03; N, 10.36; S, 8.17.

6.1.6. N-[2,5-Diethoxy-4-(3-p-tolyl-ureidomethyl)-phenyl]-methanesulfonamide (13)

According to the same procedure described for **14H**, **11** (500 mg, 1.39 mmol) was treated with 4-methylaniline (149 mg, 1.39 mmol) and triethylamine (1.40 g, 13.9 mmol) to afford 430 mg (yield 83.0%) of 1-(2,5-diethoxy-4-nitro-benzyl)-3-p-tolyl-urea (**13H**) as a white solid. According to the same procedure described for **14I**, **13H** (350 mg, 0.94 mmol) was treated with $NiCl_2 \cdot 6H_2O$ (384 mg, 1.6 mmol) and $NaBH_4$ (122 mg, 3.2 mmol) to afford 275 mg (yield 85.5%) of 1-(4-amino-2,5-diethoxy-benzyl)-3-p-tolyl-urea (**13I**) as a white solid. According to the same procedure described for **14**, **13I** (260 mg, 0.76 mmol) was treated with pyridine (65.9 mg, 0.83 mmol) and methanesulfonyl chloride (87.0 mg, 0.76 mmol) to afford 160 mg (yield 50.2%) of N-[2,5-diethoxy-4-(3-p-tolyl-ureidomethyl)-phenyl]-methanesulfonamide (**13**) as a white solid. ^{1}H NMR (400 MHz, CDCl$_3$) δ 7.10 (d, $J = 10.8$ Hz, 4H), 6.90 (d, $J = 6.8$ Hz, 1H), 6.75 (s, 1H), 4.36 (d, $J = 5.6$ Hz, 2H), 3.99 (m, 4H), 2.92 (s, 3H), 2.32 (s, 3H), 1.38 (t, $J = 6.8$ Hz, 3H), 1.30–1.26 (m, 3H). ^{13}C NMR (101 MHz, DMSO) δ 155.19, 149.66, 145.38, 137.87, 128.97, 128.57, 126.25, 125.17, 121.02, 117.81, 117.67, 113.71, 110.55, 64.61, 64.13, 40.21, 38.08, 20.21, 14.67, 14.61; Anal. ($C_{20}H_{27}N_3O_5S$): Anal. Calcd for C, 56.99; H, 6.46; N, 9.97; S, 7.61. Found: C, 56.95; H, 6.10; N, 9.94; S, 7.68.

6.1.7. N-{2,5-Diethoxy-4-[3-(4-methoxy-phenyl)-ureidomethyl]-phenyl}-methanesulfonamide (15)

According to the same procedure described for **14H**, **11** (500 mg, 1.39 mmol) was treated with m-methoxyaniline (171 mg, 1.39 mmol) and triethylamine (1.40 g, 13.9 mmol) to afford 450 mg (yield 83.3%) of 1-(2,5-diethoxy-4-nitro-benzyl)-3-(4-methoxy-phenyl)-urea (**15H**) as a white solid. According to

the same procedure described for **14I**, **15H** (400 mg, 1.03 mmol) was treated with $NiCl_2 \cdot 6H_2O$ (420 mg, 1.77 mmol) and $NaBH_4$ (134 mg, 3.53 mmol) to afford 290 mg (78.3%) of 1-(4-amino-2,5-diethoxy-benzyl)-3-(4-methoxy-phenyl)-urea (**15I**) as a white solid. According to the same procedure described for **14**, **15I** (250 mg, 0.70 mmol) was treated with Pyridine (60.5 mg, 0.77 mmol) and methanesulfonyl chloride (80.2 mg, 0.70 mmol) to afford 145 mg (47.7%) of N-{2,5-diethoxy-4-[3-(4-methoxy-phenyl)-ureidomethyl]-phenyl}-methanesulfonamide (**15**) as a white solid. ^{1}H NMR (400 MHz, CDCl$_3$) δ 7.15 (d, $J = 8.7$ Hz, 2H), 7.08 (s, 1H), 6.92–6.81 (m, 3H), 6.75 (s, 1H), 4.35 (s, 2H), 4.03 (q, $J = 6.9$ Hz, 2H), 3.96 (q, $J = 6.9$ Hz, 2H), 3.79 (s, 3H), 2.92 (s, 3H), 1.38 (t, $J = 6.9$ Hz, 3H), 1.26 (t, $J = 6.9$ Hz, 3H). ^{13}C NMR (101 MHz, DMSO) δ 155.35, 153.96, 149.60, 145.40, 133.55, 126.32, 125.04, 119.42 (2C), 113.88(2C), 113.58, 110.57, 64.56, 64.06, 55.12, 40.10, 38.10. 14.67, 14.62; Anal. ($C_{20}H_{27}N_3O_6S$): Anal. Calcd for C, 54.90; H, 6.22; N, 9.60; S, 7.33. Found: C, 56.47; H, 5.87; N, 9.68; S, 7.34.

6.1.8. N-{2,5-Diethoxy-4-[3-(3-methoxy-phenyl)-ureidomethyl]-phenyl}-methanesulfonamide (16)

According to the same procedure described for **14H**, **11** (500 mg, 1.39 mmol) was treated with p-methoxyaniline (171 mg, 1.39 mmol) and triethylamine (1.40 g, 13.9 mmol) to afford 445 mg (yield 82.4%) of 1-(2,5-diethoxy-4-nitro-benzyl)-3-(3-methoxy-phenyl)-urea (**16H**) as a white solid. According to the same procedure described for **14I**, **16H** (400 mg, 1.03 mmol) was treated with $NiCl_2 \cdot 6H_2O$ (420 mg, 1.77 mmol) and $NaBH_4$ (134 mg, 3.53 mmol) to afford 305 mg (yield 80.9%) of 1-(4-amino-2,5-diethoxy-benzyl)-3-(3-methoxy-phenyl)-urea (**16I**) as a white solid. According to the same procedure described for **14**, **16I** (260 mg, 0.64 mmol) was treated with pyridine (55.6 mg, 0.70 mmol) and methanesulfonyl chloride (73.3 mg, 0.64 mmol) to afford 170 mg (yield 54.8%) of N-{2,5-diethoxy-4-[3-(3-methoxy-phenyl)-ureidomethyl]-phenyl}-methanesulfonamide (**16**) as a white solid. ^{1}H NMR (400 MHz, CDCl$_3$) δ 7.19 (t, $J = 8.1$ Hz, 1H), 7.10 (s, 1H), 6.94 (s, 1H), 6.90 (s, 1H), 6.77 (d, $J = 12.0$ Hz, 2H), 6.64 (d, $J = 8.2$ Hz, 1H), 4.37 (s, 2H), 4.07–3.93 (m, 4H), 3.76 (s, 3H), 2.92 (s, 3H), 1.38 (t, $J = 7.0$ Hz, 3H), 1.32 (t, $J = 6.6$ Hz, 3H). ^{13}C NMR (101 MHz, DMSO) δ 155.37, 154.01, 149.64, 145.38, 133.58, 126.34, 125.14, 119.48(2C), 113.91(2C), 113.68, 110.55, 64.61, 64.13, 55.15, 40.22, 38.10, 14.67, 14.61; Anal. ($C_{20}H_{27}N_3O_6S$): Anal. Calcd for: C, 54.90; H, 6.22; N, 9.60; S, 7.33. Found: C, 54.76; H, 6.02; N, 9.66; S, 7.44.

6.1.9. N-{4-[3-(3,4-Dimethoxy-phenyl)-ureidomethyl]-2,5-diethoxy-phenyl}-methanesulfonamide (17)

According to the same procedure described for **14H**, **11** (500 mg, 1.39 mmol) was treated with 3,4-dimethoxyaniline (213 mg, 1.39 mmol) and triethylamine (1.40 g, 13.9 mmol) to afford 440 mg (yield 75.6%) of 1-(2,5-diethoxy-4-nitro-benzyl)-3-(3,4-dimethoxy-phenyl)-urea (**17H**) as a white solid. According to the same procedure described for **14I**, **17H** (400 mg, 0.95 mmol) was treated with $NiCl_2 \cdot 6H_2O$ (388 mg, 1.63 mmol) and $NaBH_4$ (124 mg, 3.26 mmol) to afford 300 mg (80.9%) of 1-(4-amino-2,5-diethoxy-benzyl)-3-(3,4-dimethoxy-phenyl)-urea (**17I**) as a white solid. According to the same procedure described for **14**, **17I** (260 mg, 0.64 mmol) was treated with pyridine (55.6 mg, 0.70 mmol) and methanesulfonyl chloride (73.3 mg, 0.64 mmol) to afford 170 mg (yield 54.8%) of N-{4-[3-(3,4-dimethoxy-phenyl)-ureidomethyl]-2,5-diethoxy-phenyl}-methanesulfonamide (**17**) as a white solid. ^{1}H NMR (400 MHz, CDCl$_3$) δ 7.08 (s, 1H), 6.94 (s, 1H), 6.89 (s, 1H), 6.82–6.73 (m, 2H), 6.70 (d, $J = 8.1$ Hz, 1H), 6.56 (s, 1H), 4.36 (s, 2H), 3.99 (ddd, $J = 25.1, 13.6, 6.7$ Hz, 4H), 3.84 (d, $J = 12.4$ Hz, 6H), 2.92 (s, 3H), 1.38 (t, $J = 6.7$ Hz, 3H), 1.27 (t, $J = 5.6$ Hz, 3H); ^{13}C NMR (101 MHz, DMSO) δ 155.28, 149.65,

ARTICLE IN PRESS

Y. Du et al./Bioorg. Med. Chem. xxx (2015) xxx–xxx   7

148.89, 145.38, 143.63, 134.30, 126.32, 125.15, 113.67, 112.89, 110.54, 109.69, 103.80, 64.63, 64.12, 56.03, 55.37, 40.22, 38.10, 14.67, 14.61; Anal. ($C_{21}H_{29}N_3O_7S$): Anal. Calcd for C, 53.95; H, 6.26; N, 8.99; S, 6.86. Found: C, 53.69; H, 6.25; N, 8.87; S, 7.17.

6.1.10. N-[4-(3-Benzyl-ureidomethyl)-2,5-diethoxy-phenyl]-methanesulfonamide (18)

According to the same procedure described for **14H**, **11** (500 mg, 1.39 mmol) was treated with benzylamine (149 mg, 1.39 mmol) and triethylamine (1.40 g, 13.9 mmol) to afford 420 mg (81.1%) of 1-benzyl-3-(2,5-diethoxy-4-nitro-benzyl)-urea (**18H**) as a white solid. According to the same procedure described for **14I**, **18H** (400 mg, 1.07 mmol) was treated with $NiCl_2 \cdot 6H_2O$ (438 mg, 1.84 mmol) and $NaBH_4$ (140 mg, 3.68 mmol) to afford 300 mg (yield 81.5%) of 1-(4-amino-2,5-diethoxy-benzyl)-3-benzyl-urea (**18I**) as a white solid. According to the same procedure described for **14**, **18I** (250 mg, 0.73 mmol) was treated with pyridine (63.3 mg, 0.80 mmol) and methanesulfonyl chloride (83.6 mg, 0.73 mmol) to afford 170 mg (yield 55.9%) of N-[4-(3-benzyl-ureidomethyl)-2,5-diethoxy-phenyl]-methanesulfonamide (**18**) as a white solid. ^{1}H NMR (400 MHz, DMSO) δ 8.80 (s, 1H), 7.34 –7.16 (m, 5H), 6.87 (s, 1H), 6.84 (s, 1H), 6.51 (t, J = 6.0 Hz, 1H), 6.23 (t, J = 5.6 Hz, 1H), 4.20 (t, J = 7.5 Hz, 2H), 4.16 (d, J = 5.9 Hz, 2H), 3.94 (m, 6.9 Hz, 4H), 2.92 (s, 3H), 1.31 (m J = 6.9, 3.7 Hz, 6H). ^{13}C NMR (101 MHz, DMSO) δ 155.19, 149.66, 145.38, 137.87, 128.97, 128.57, 126.25, 125.17, 121.02 (s), 117.81, 117.67, 113.71, 110.55, 64.61, 64.13, 40.21, 38.08, 20.21, 14.67, 14.61; Anal. ($C_{20}H_{27}N_3O_5S$): Anal. Calcd for C, 56.99; H, 6.40; N, 9.97; S, 7.61. Found: C, 56.73; H, 6.46; N, 10.04; S, 8.02.

6.2. PTP1B and related PTPs biological assay

PTP1B inhibitory activities were measured as previously described with minor revision.[30,31] Briefly, PTP1B hydrolyzes pNPP to pNP that can be detected at 405 nm. Test compounds were predispensed in 96-well microplates as 1.0 µL aliquots per well in 100% DMSO. The PTP1B enzymatic assay was carried out in a total volume of 100 µL per well in assay plates with 30 nM recombinant PTP1B protein, 2 mM *p*-nitrophenylphosphonic acid (pNPP), 1 mM dithiothreitol and 1 mM EDTA (pH 6.5). After 30 min incubation at 37 °C, the reaction was terminated by addition of 2.5 M NaOH. The amount of hydrolysis product, pNP, was monitored by detection of the absorbance at 405 nm. IC$_{50}$ values were calculated by Graphpad Prism 5.0 software (Logit method). To determine cross-reactivity of test compounds, the same protocol was followed for inhibition assay with TCPTP.

To study the inhibition on the other PTPs family members, SHP1, SHP2 and LAR assays were performed according to procedures described previously.[32]

6.3. Characterization of the inhibitor on enzyme kinetics

To characterize the inhibitor of PTP1B, the assay was carried out in a 100 µL system containing 50 mM MOPS, pH 6.5, 30 nM PTP1B, pNPP in 2-fold dilution from 64 mM, and different concentrations of the inhibitor.[33] In the presence of the competitive inhibitor, the Michaelis–Menten equation is described as $1/v = (K_m/[V_{max}[S]])(1 + [I]/K_i) + 1/V_{max}$, where K_m is the Michaelis constant, v is the initial rate, V_{max} is the maximum rate, and $[S]$ is the substrate concentration. The K_i value was obtained by the linear replot of apparent K_m/V_{max} (slope) from the primary reciprocal plot versus the inhibitor concentration $[I]$ according to the equation $K_m/V_{max} = 1 + [I]/K_i$.

6.4. Effect of PTP1B inhibitors on the phosphorylation level of IR in transfected CHO cells

CHO cells were cultured in the presence of F12 supplemented with 10% FBS and seeded 24 h before transfection in 6 cm dish

(6×10^5 cells per dish). 2 µg of the human IR plasmid was introduced into cells by using FuGENE 6 transfection reagent (Roche) according to the manufacturer's protocol. Cells were transfected for 8 h, and harvested with 0.05% trypsin and 0.02% EDTA prior to reseeding onto a 6-well plate. After 24 h with 5% CO$_2$ at 37 °C, CHO cells serum free starved for 2 h were incubated with compounds for 4 h, then 10 nM insulin was added stimulation for 10 min before harvested.

For total protein extraction, CHO cells were lysed in the ice-cold buffer A (1% Triton X-100, 100 mM sodium pyrophosphate, 2 mM phenylmethylsulfonyl fluoride (PMSF), 50 mM HEPES, pH7.4) and centrifuged at 15,000g for 20 min at 4 °C. Supernatants were collected and stored at −80 °C. For subcellular fractionation, cells were lysed in buffer B (0.25 M sucrose, 2 mM EDTA, 1 mM phenyl-methylsulfonyl fluoride (PMSF) and 10 mM Tris-HCl, pH 7.4). The lysates were centrifuged at 750g for 15 min, and the supernatants were centrifuged at 12,000g for 20 min to isolate the crude plasma membrane fraction as the pellets. Equal amount of protein from each sample were denatured and subjected to SDS-PAGE and blotted on PVDF membrane, which was incubated for 2 h at room temperature with blocking buffer (5% non-fat milk, 0.1% Tween 20, in TBS, pH 7.6) and then probed with primary antibodies (PY-20 and β-actin) overnight at 4 °C. After incubation with the appropriate secondary antibodies, the immunoreactive band was detected by an ECL Western blotting detection system (GE Healthcare).[34]

6.5. Molecular docking

The crystal structure of the progesterone binding domain of PTP1B in complex with compound **1** was retrieved from the RCSB Protein Data Bank (PDB entry 2CNE). All the docking simulations of the studied compound**s** within the binding pocket of PTP1B have been performed using Surflex docking program (Sybyl X 1.0) with the default settings.

Acknowledgment

Supplementary data

Supplementary data associated with this article can be found, in the online version, at http://dx.doi.org/10.1016/j.bmc.2015.05.032. These data include MOL files and InChiKeys of the most important compounds described in this article.

References and notes

1. Asante-Appiah, E.; Kennedy, B. P. *Am. J. Physiol. Endocrinol. Metab.* **2003**, *284*, E663.
2. Cook, W. S.; Unger, R. H. *Dev. Cell.* **2002**, *2*, 385.
3. Byon, J. C.; Kusari, A. B.; Kusari, J. *Mol. Cell. Biochem.* **1998**, *182*, 101.
4. Combs, A. P. *J. Med. Chem.* **2010**, *53*, 2333.
5. Szczepankiewicz, B. G.; Liu, G.; Hajduk, P. J.; Abad-Zapatero, C.; Pei, Z.; Xin, Z.; Lubben, T. H.; Trevillyan, J. M.; Stashko, M. A.; Ballaron, S. J.; Liang, H.; Huang, F.; Hutchins, C. W.; Fesik, S. W.; Jirousek, M. R. *J. Am. Chem. Soc.* **2003**, *125*, 4087.
6. Combs, A. P.; Yue, E. W.; Bower, M.; Ala, P. J.; Wayland, B.; Douty, B.; Takvorian, A.; Polam, P.; Wasserman, Z.; Zhu, W.; Crawley, M. L.; Pruitt, J.; Sparks, R.; Glass, B.; Modi, D.; McLaughlin, E.; Bostrom, L.; Li, M.; Galya, L.; Blom, K.; Hillman, M.; Gonneville, L.; Reid, B. G.; Wei, M.; Becker-Pasha, M.; Klabe, R.; Huber, R.; Li, Y.; Hollis, G.; Burn, T. C.; Wynn, R.; Liu, P.; Metcalf, B. *J. Med. Chem.* **2005**, *48*, 6544.
7. Puius, Y. A.; Zhao, Y.; Sullivan, M.; Lawrence, D. S.; Almo, S. C.; Zhang, Z.-Y. *Proc. Natl. Acid. Sci. U.S.A.* **1997**, *94*, 13420.
8. Lau, C. K.; Bayly, C. I.; Gauthier, J. Y.; Li, C. S.; Therien, M.; Asante-Appiah, E.; Cromlish, W.; Boie, Y.; Forghani, F.; Desmarais, S.; Wang, Q.; Skorey, K.; Waddleton, D.; Payette, P.; Ramachandran, C.; Kennedy, B. P.; Scapin, G. *Bioorg. Med. Chem. Lett.* **2004**, *14*, 1043.
9. Low, J.-L.; Chai, C. L. L.; Yao, S. Q. *Antioxid. Redox. Signal.* **2014**, *20*, 2225.

10. Liu, G.; Xin, Z.; Liang, H.; Abad-Zapatero, C.; Hajduk, P. J.; Janowick, D. A.; Szczepankiewicz, B. G.; Pei, Z.; Hutchins, W. C.; Ballaron, S. J.; Stashko, M. A.; Lubben, T. H.; Berg, C. E.; Rondinone, C. M.; Trevillyan, J. M.; Jirousek, M. R. *J. Med. Chem.* **2003**, *46*, 3437.

11. Xin, Z.; Liu, G.; Abad-Zapatero, C.; Pei, Z.; Szczepankiewicz, B. G.; Li, X.; Zhang, T.; Hutchins, C. W.; Hajduk, P. J.; Ballaron, S. J.; Stashko, M. A.; Lubben, T. H.; Trevillyan, J. M.; Jirousek, M. R. *Bioorg. Med. Chem. Lett.* **2003**, *13*, 3947.

12. Liu, G.; Xin, Z.; Pei, Z.; Hajduk, P. J.; Abad-Zapatero, C. W.; Hutchins, C.; Zhao, H.; Lubben, T. H.; Ballaron, S. J.; Haasch, D. L.; Kaszubska, W.; Rondinone, C. M.; Trevillyan, J. M.; Jirousek, M. R. *J. Med. Chem.* **2003**, *46*, 4232.

13. Wilson, D. P.; Wan, Z.-K.; Xu, W.-X.; Kirincich, S. J.; Follows, B. C.; Joseph-McCarthy, D.; Foreman, K.; Moretto, A.; Wu, J.; Zhu, M.; Binnun, E.; Zhang, Y.-L.; Tam, M.; Erbe, D. V.; Tobin, J.; Xu, X.; Leung, L.; Shilling, A.; Tam, S. Y.; Mansour, T. S.; Lee, J. *J. Med. Chem.* **2007**, *50*, 4681.

14. Combs, A. P.; Zhu, W.; Crawley, M. L.; Glass, B.; Polam, P.; Sparks, R. B.; Modi, D.; Takvorian, A.; McLaughlin, E.; Yue, E. W.; Wasserman, Z.; Bower, M.; Wei, M.; Rupar, M.; Ala, P. J.; Reid, B. M.; Ellis, D.; Gonneville, L.; Emm, T.; Taylor, N.; Yeleswaram, S.; Li, Y.; Wynn, R.; Burn, T. C.; Hollis, G.; Liu, P. C.; Metcalf, B. *J. Med. Chem.* **2006**, *49*, 3774.

15. Douty, B.; Wayland, B.; Ala, P. J.; Bower, M. J.; Pruitt, J.; Bostrom, L.; Wei, M.; Klabe, R.; Gonneville, L.; Wynn, R.; Burn, T. C.; Liu, P. C.; Combs, A. P.; Yue, E. W. *Bioorg. Med. Chem. Lett.* **2008**, *18*, 66.

16. Salmeen, A.; Andersen, J. N.; Myers, M. P.; Tonks, N. K.; Barford, D. *Mol. Cell.* **2000**, *6*, 1401.

17. Iversen, L. F.; Andersen, H. S.; Branner, S.; Mortensen, S. B.; Peters, G. H.; Norris, K.; Olsen, O. H.; Jeppesen, C. B.; Lundt, B. F.; Ripka, W.; Moller, K. B.; Moller, N. P. *J. Biol. Chem.* **2000**, *275*, 10300.

18. Ala, P. J.; Gonneville, L.; Hillman, M.; Becker-Pasha, M.; Yue, E. W.; Douty, B.; Wayland, B.; Polam, P.; Crawley, M. L.; McLaughlin, E.; Sparks, R. B.; Glass, B.; Takvorian, A.; Combs, A. P.; Burn, T. C.; Hollis, G. F.; Wynn, R. *J. Biol. Chem.* **2006**, *281*, 38013.

19. Zhao, Y.; Shirai, Y.; Slepkov, A. D.; Cheng, L.; Alemany, L. B.; Sasaki, T.; Hegmann, F. A.; Tour, J. M. *Chem. Eur. J.* **2005**, *11*, 3643.

20. Shchekotikhin, A. E.; Makarov, I. G.; Buyanov, V. N.; Preobrazhenskaya, M. N. *Chem. Heterocycl. Compd.* **2005**, *41*, 914.

21. Makhija, Mahindra T.; Kasliwal, Rajesh T.; Kulkarnia, Vithal M.; Neamati, Nouri *Bioorg. Med. Chem.* **2004**, *12*, 2317.

22. Weingarth, Markus; Raouafi, Noureddine; Jouvelet, Benjamin; Duma, Luminita *Chem. Commun.* **2008**, 5981.

23. Liu, Qi; Luedtke, Nathan W.; Tor, Yitzhak *Tetrahedron Lett.* **2001**, *42*, 1445.

24. Diss, Maria L.; Kennan, Alan J. *Biopolymers* **2007**, *86*, 276.

25. Takeuchi, Yasuo; Oda, Toshiaki; Chang, Ming-rong; Okamoto, YoKo; Ono, Junko, et al. *Chem. Pharm. Bull.* **1997**, *45*, 406.

26. Panzhinskiy, E.; Ren, J.; Nair, S. *Curr. Med. Chem.* **2013**, *20*, 2609.

27. Zinker, B. A.; Rondinone, C. M.; Trevillyan, J. M.; Gum, R. J.; Clampit, J. E.; Waring, J. F.; Xie, N.; Wilcox, D.; Jacobson, P.; Frost, L.; Kroeger, P. E.; Reilly, R. M.; Koterski, S.; Opgenorth, T. J.; Ulrich, R. G.; Crosby, S.; Butler, M.; Murray, S. F.; McKay, R. A.; Bhanot, S.; Monia, B. P.; Jirousek, M. R. *Proc. Natl. Acid. Sci. U.S.A.* **2002**, *99*, 11357.

28. Fukuda, S.; Ohta, T.; Sakata, S.; Morinaga, H.; Ito, M.; Nakagawa, Y.; Tanaka, M.; Matsushita, M. *Diabetes Obes. Metab.* **2010**, *12*, 299.

29. Maeda, A.; Kai, K.; Ishii, M.; Ishii, T.; Safranal, Akagawa M. *Mol. Nutr. Food Res.* **2014**, *58*, 1177.

30. Otake, K.; Azukizawa, S.; Fukui, M.; Kunishiro, K.; Kamemoto, H.; Kanda, M.; Miike, T.; Kasai, M.; Shirahase, H. *Bioorg. Med. Chem.* **2012**, *20*, 1060.

31. Lakshminarayana, N.; Prasad, Y. R.; Gharat, L.; Thomas, A.; Narayanan, S.; Raghuram, A.; Srinivasan, C. V.; Gopalan, B. *Eur. J. Med. Chem.* **2010**, *45*, 3709.

32. Shi, L.; Yu, H. P.; Zhou, Y. Y.; Du, J. Q.; Shen, Q.; Li, J. Y.; Li, J. *Acta Pharmacol. Sin.* **2008**, 29.

33. Zhi, Y.; Gao, L. X.; Jin, Y.; Tang, C. L.; Li, J. Y.; Li, J.; Long, Y. Q. *Bioorg. Med. Chem.* **2014**, *22*, 3670.

34. Chen, L.; Li, Q. Y.; Shi, X. J.; Mao, S. L.; Du, Y. L. *J. Agric. Food Chem.* **2013**, *61*, 10714.